Tellus (1983), *35A*, 398–416

Further numerical experiments on tropical waves

By J. A. ADEJOKUN and T. N. KRISHNAMURTI, *Department of Meteorology, Florida State University, Tallahassee, Florida 32306, USA*

(Manuscript received July 28, 1982; in final form February 4, 1983)

ABSTRACT

A series of experiments, designed to study single level predictions with a barotropic and a primitive equation (PE) model, essentially following Krishnamurti et al. (1980), has been carried out for June to September 1979 utilizing the FGGE (First GARP Global Experiment) data sets. The level chosen for this study is the 700 mb, covering a domain extending from 100° W to 38° E and 25° S to 45° N. Most of the waves of 1979, identified by Frank and Clark (1980), were investigated. Because these waves were not always well defined in the analysis at 700 mb, a wave anomaly pattern, prepared from Reed et al.'s (1977) composite African wave model, was carefully inserted in the respective locations of the waves. Major improvement in the tracking and passage of waves resulted from the merging of the African and easterly wave models into the broadscale flow patterns defined by the FGGE data sets. This study includes an analysis of the prediction errors. In this context the root mean square vector wind errors and the anomaly correlations are presented. The results of some 52 experiments show that the simple model based on the conservation of vorticity, performs better than persistence up to 2 days, while the next model, which is based on the conservation of potential vorticity, performs better than persistence up to 4 days. In general, very useful forecasts up to 2 days are possible with the single level PE model.

1. Introduction

The purpose of this present study is to establish the predictive capabilities of simple tropical models that use the conservation laws of absolute and potential vorticity as the guiding principle, using the best available data sets during the global experiment. This is done by carrying out a very large number of prediction experiments with the respective models and the evaluation is here determined from the measures of standard statistical errors such as root mean square (RMS) error and the anomaly correlation coefficient. This study also provides a comparison of some of these prediction errors with those from the persistence of the tropical flow fields.

An objective of this study is to assess how well the two single level models handle the passage and intensity of African waves over the Atlantic ocean. In this respect, this is an extension of the results obtained with GATE data by Krishnamurti et al. (1980). The predictability of the forecast models, beyond which their operational value is limited, is also addressed here.

A brief mathematical background of the barotropic and the single level PE models, used in this study, is given in Section 2. Section 3 addresses the data sets and the analysis procedures of the present study. Results of the 52 prediction experiments are discussed in Section 4.

Only a limited amount of work has been done previously with numerical weather prediction models for operational weather prediction in low latitudes. In particular the forecasting of the movement of tropical waves or disturbances by numerical means has so far not received the attention it deserves. The main reasons for this include the hitherto lack of adequate and reliable observations, as well as the difficulty in modelling the tropical flow patterns. Weak horizontal variations of the weather variables in, and the complexity of the physics describing the dynamics of these regions are a few of the problems contributing to this difficulty.

The importance of the African wave disturbances to the weather of the tropical Atlantic, Caribbean and the southeastern coasts of the United States during the northern summer has been an established fact since the work of Piersig (1936), who used charts of the Netherlands Institute from 1881 to 1911 to study the behavior of "pressure disturbances which form in the trade wind belt of the eastern North Atlantic". Dunn (1940) also mentioned "tracks of isallobaric waves" moving along the trades current over the Atlantic. These westward propagating disturbances have since been shown to be the major sources of many tropical depressions and hurricanes. Fritz (1962) tracked hurricane Anna from 12° N 43° W—i.e. from the middle Atlantic ocean; however he gave evidence for a low pressure area which originated over Africa. Frank (1970) has shown that although only a small number of waves ultimately intensify, African waves account for about half of the tropical cyclones of the Atlantic ocean.

Erickson (1963), Carlson (1969a, b), Burpee (1972) and Adefolalu (1974) used some surface and upper air observations, supplemented later by satellite photographs, to define the origin, structure and motion of the African waves. Later, other authors, Pedgeley and Krishnamurti (1976); Reed, Norquist and Recker (1977), and several others utilized the African and the GATE (GARP Atlantic Tropical Experiment) data sets to construct the structure, and properties of monsoon cyclones and African wave disturbances over West Africa. (A list of acronyms is provided in Table 1.)

Krishnamurti et al. (1980) carried out a number of experiments with single level models utilizing the special observations from GATE with promising results on the passage of African waves. In this study, these efforts are extended with the more complete data sets from the global experiment—i.e. FGGE level IIIb data.

Table 1. *List of acronyms*

NOAA	National Oceanic and Atmospheric Administration
FGGE	First GARP Global Experiment
GARP	Global Atmospheric Research Programme
GATE	GARP Atlantic Tropical Experiment
RMS	Root Mean Square
PE	Primitive Equation
ECMWF	European Centre for Medium Range Weather Forecast

Thompson et al. (1979) and Krishnamurti et al. (1979a), among others, have shown that the maximum amplitude of the African waves occurs near the 700 mb level. They also observed that barotropic energy exchanges, $\langle K_z \cdot K_E \rangle$, as well as the intensity of the lower tropospheric West African jet are largest near the 700 mb level. In addition, the level of non-divergence seems to be close to 700 mb, especially over the GATE region. For the above-mentioned reasons, the 700 mb level has been chosen for the present series of single level experiments.

2. The models

2.1 *The tropical barotropic model*

2.1.1. *Basic equation.* Using the principle of conservation of absolute vorticity, Krishnamurti and Pearce (1977) designed a tropical barotropic model. This is expressed by the familiar relation on the streamfunction ψ

$$\frac{\partial}{\partial t}\nabla^2\psi = -\mathrm{J}(\psi, \nabla^2\psi) - \beta\frac{\partial\psi}{\partial x} \qquad (1)$$

where J is the Jacobian operator and $\beta = \partial f/\partial y$. A list of symbols is provided in Table 2.

Eq. (1) forms the basic framework of the tropical barotropic model used in this study.

Table 2. *List of symbols*

c	phase speed
f	coriolis parameter
g	earth's gravity
h	terrain height
u	zonal wind component
v	meridional wind component
z	free surface height
K	kinetic energy
J	Jacobian operator
∇^2	Laplacian operator
D/Dt	Lagrangian operator
β	meridional deviation of the earth's vorticity
ζ	relative vorticity
ζ_a	absolute vorticity
ζ_p	potential vorticity
ϕ	latitude
ψ	streamfunction
$\bar{(\ )}$	zonal average
$\langle K_z \cdot K_E \rangle$	barotropic energy conversion (zonal kinetic to eddy kinetic)
E_T	total energy parameter

2.1.2. *Features of the barotropic model.* This model is constructed to conserve not only the average absolute vorticity, $\bar{\zeta}_a$, in a domain but also the square of the mean absolute vorticity, $\bar{\zeta}_a^2$, as well as the domain average kinetic energy, $\bar{K}$. The invariance of $\bar{\zeta}_a^2$ and $\bar{K}$ are important properties if the model is to give realistic forecast flows. Another property of the barotropic model is its capability for energy exchanges, $\langle K_z \cdot K_E \rangle$, during barotropically unstable shear flows. Other features of the model include the use of the so-called "Arakawa Jacobian" for the finite-differencing of the advective term $J(\psi, \nabla^2\psi)$, following Arakawa (1966), and an Euler backward time-differencing scheme as suggested by Matsuno (1966). For this study a time step of 2700 s was utilized. This time step was determined by the Courant, Levy, Fredrick criterion to a grid distance of 1° latitude/longitude mesh. For the finite difference representation of ∇^2, a standard second-order Laplacian was utilized.

2.1.3. *Computation of streamfunction.* In the barotropic model used for this study, the initial streamfunction has been defined from the initial horizontal motion field following Krishnamurti (1969). Subsequent computations of the streamfunction for the 96 h of integration are determined using the Tukey's Fast-Fourier transform method following Hockney (1965). This is a much faster method than the usual relaxation of the relative vorticity, $\nabla^2\psi$.

2.1.4. *Boundary conditions and smoothing.* As boundary conditions, the domain has been extended in the zonal direction by adding six extra rows of grid points beyond the analysis domain using a linear interpolation. This removes the east–west boundaries and ensures a smooth cyclic continuity of the analysis. At the northern and southern boundaries the initial streamfunction is made to vary in the zonal direction while the tendency of the streamfunction $\partial\psi/\partial t$ is set to zero at these two walls during the integration. In effect we have an open boundary with $u = v =$ constant at the north and south boundaries.

Apart from the smoothings implied in the finite differencing schemes used for the time tendency and the advective terms of the model no other smoothing is found necessary.

2.2. *One-level PE model*

2.2.1. *Basic equations.* The following three equations describe the model:

Equation of motion:

$$\frac{Du}{Dt} = fv - g\frac{\partial}{\partial x}(z + h) \tag{2}$$

$$\frac{Dv}{Dt} = -fu - g\frac{\partial}{\partial y}(z + h). \tag{3}$$

Mass continuity equation:

$$\frac{Dz}{Dt} = -z\left[\frac{\partial u}{\partial x} + \frac{\partial v}{\partial y}\right], \tag{4}$$

where z is the height of a free surface and h is a smoothed mountain height.

2.2.2. *Features of the one-level PE model.* The invariants of the model include the domain averaged potential vorticity, $\bar{\zeta}_p = \overline{(\zeta + f)/z}$ and all its powers $(\overline{\zeta_p^n})$, a total energy parameter, $E_T = \overline{z(K + gz/2 + gh)}$, and the mean height of the free surface, $\bar{z}$. While the model conserves the above-mentioned invariants for a closed domain, in this study the northern and southern boundaries have been kept open to allow for a more realistic flow. In spite of this it was found that the three invariants mentioned above remained within 2% of the initial values throughout the 96-h integration.

In order to assure a near invariance of the domain invariants mentioned above, and at the same time control non-linear computational instability, the semi-Lagrangian advection scheme as proposed by Krishnamurti (1962) and Mathur (1970) is used in the treatment of the horizontal advective terms of the model. In this scheme the dynamics of the PE is used to determine the origin of a parcel arriving at a grid point in a time step, Δt. For this study a time step of 600 s has been utilized.

2.3.3. *Boundary conditions.* The boundary conditions used for this model are as described by Krishnamurti et al. (1980). Briefly, the domain has a cyclic continuity in the zonal direction by providing an artificial region, extending for about 1300 km at the eastern end of the observational domain. This 1300 km region is created only for the initial u and v fields while the geopotential, z, over the entire cyclic domain is obtained by solving the non-linear balance equation. At the northern and southern boundaries, the time tendencies $\partial u/\partial t$ and $\partial v/\partial t$, are set to zero even though the boundaries are kept open. Thus u, v, z are kept

constant at the north and south boundaries. As a result of these boundary conditions large inflow–outflow discontinuities develop at these lateral boundaries. In order to reduce these discontinuities a smoothing of the form:

$$F_{i,j} = \alpha(F_{i,j}) + \tfrac{1}{2}(1-\alpha)\,(F_{i,j+1} + F_{i,j-1})$$

is applied. F is any variable and α is a smoothing coefficient, $= 0{\cdot}95$.

2.2.4. *Treatment of the bottom topography, h, and the mean height of the free surface, $\bar{z}$.* Krishnamurti et al. (1977) has discussed the importance of mountains in the one-level PE model. In that study it was shown that forecast experiments run (using GATE data) with terrain heights included, give results closer to the observed flow than those run without terrain.

It is important that a free surface mean height be assigned in the one-level PE since z, the height of the free surface is made up of the mean height $\bar{z}$ and a perturbation portion z'

i.e. $z = \bar{z} + z'$

From the shallow water equations (eqs. 2, 3 and 4) it can be shown that $\bar{z}$ is related to the wave phase speed, c, by the relationship

$$c - \bar{u} = \pm\sqrt{g\bar{z}}$$

It follows then that the wave phase speed is proportional to the mean height of the free surface.

For the mean height of the free surface, $\bar{z}$, a value of 2000 meters has been utilized in this study. This is in line with earlier studies by Williamson (1976), who showed that values of $\bar{z}$ smaller than the actual mean values of the depth of the pressure surface slow down the waves and give improved forecasts of the shallow water equation. Further to this, Ploshay (1977) has shown that in the GATE area, a value of 2000 meters for the mean free surface height gives most realistic phase speeds and amplitudes of the African waves.

Because of the reduced mean free surface height, the terrain heights extracted from Gates and Nelson (1975), and used in this study (see paragraph 3.1), have to be further smoothed in order to avoid unrealistic wave phase speeds. In the experiments performed, it was necessary to scale down and smooth the mountain heights to less than one-tenth of their values especially in the south-western part of the domain where the high Andes mountains were initially producing very high values of the motion fields.

3. Data and analysis procedure

3.1. *Data*

The data used in this study comprise of

(a) The FGGE Level IIIb wind data at the 850 and 700 mb, from the European Centre for Medium Range Weather Forecast (ECMWF),

(b) the high resolution satellite cloud motion vectors over the Atlantic ocean, derived by the University of Wisconsin on the McIDAS system.

(c) smoothed mountain heights obtained from Gates and Nelson (1975). The treatment of this parameter in the PE model has been described earlier.

The period covered in this study is from June 16, 1979 to September 15, 1979 for the observation time 1200 GMT each day. The 1200 GMT analysis includes low cloud motion vectors between 0600 GMT and 1800 GMT for each day.

The domain of this study is from 25° S to 45° N and from 100° W to 38° E, while the horizontal mesh size is 1° latitude/1° longitude for the barotropic model and 2° latitude/2° longitude for the one-level PE model. The difference in spacial resolution is an attempt to considerably reduce the computer time and high cost of running each experiment with the one-level PE model.

3.2. *Analysis procedure*

The 850 mb and 700 mb grid point values of the u and v components used in this study are results of objectively analysed fields of the original FGGE observations by the ECMWF. The ECMWF analysis does not include the high resolution cloud motion vectors on most days. In order to incorporate and thereby fully utilize the cloud motion vectors, a reanalysis was felt necessary. The method used here follows the method proposed by Krishnamurti et al. (1979). The wind shear between 850 mb and 700 mb is assumed to be given, i.e. in the ECMWF analysis. A reanalysis of the 850 mb motion field is first made with all available data. Next, we add the shear field to reconstruct the 700 mb analysis. The following steps were followed. First, the shears, Δu and Δv, between the 700 mb and 850 mb levels were calculated for each grid point. The 850 ECMWF analysis and the high resolution cloud motion vectors were merged together and objectively analysed to produce a final 850 mb field. The details of the objective analysis

method used are described in Tripoli and Krishnamurti (1975) and are not reviewed here. Finally, the shears, Δu and Δv, at each grid point are added to the new 850 mb u and v fields to give the new 700 mb u and v fields. These 700 mb u and v fields form the basic data used for this study.

3.3. *Initial state tropical wave identification*

In order to effectively study how well the models handle the passage of African waves, twenty-six waves identified by Frank et al. (1980), between June 15, and September 15, 1979, were tagged for the present investigation. In spite of the efforts put into obtaining a detailed 700 mb analysis as described in paragraph 3·2 above, most of the waves identified by Frank were still not reasonably well defined. For a more realistic initial state of the African wave, therefore, a 700 mb composite easterly wave anomaly, following Reed et al. (1977), (see Fig. 1), was carefully inserted in the respective locations of the waves as determined by Frank's study. Here the anomaly implies a perturbation wind field from Reed et al. (1977) composite, where the zonal mean composited flows had been removed. The premise here is that the larger scale data sets define the broad scale horizontal shear which is important for the future evolution of the waves themselves. A limitation of this approach is that the variability of easterly waves anomaly from one case to the next is ignored. We found that this was inevitable simply because the density of FGGE observations were inferior to those during GATE over the eastern Atlantic ocean. It is to be noted here that Frank used satellite photographs and time sections to determine the approximate locations of the waves. As a result of this merging of the easterly wave anomaly model with the African wave, major improvement in the definition, tracking and passage of the tagged African waves ensued. Fig. 2 illustrates a typical objectively analysed 700 mb initial state streamlines (solid thin lines) and isotachs (dotted thin lines). Five tropical waves (heavy dotted lines) may be identified in this illustration.

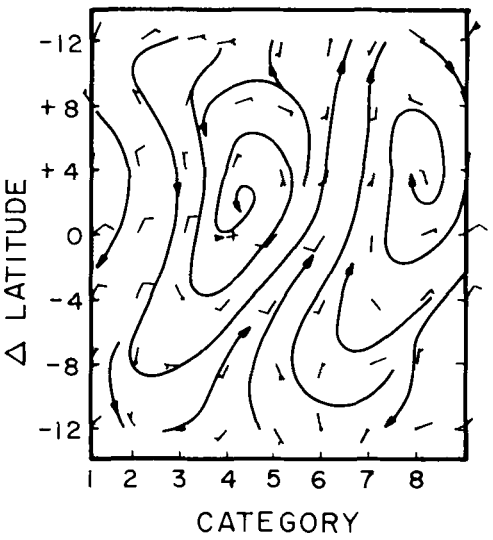

Fig. 1. Streamlines for perturbed wind field (Wave Anomaly) at 700 mb—copied from Reed et al. (1977). A category width represents about 3° of longitude. The cross denotes disturbance center. "Zero" latitude on the Δ latitude scale corresponds to average latitude of disturbance center. One full barb corresponds to 5 m s^{-1}, one half barb to 2.5 m s^{-1} and no barb to 1 m s^{-1}.

4. Results of prediction experiments

Fifty-two 96-h prediction experiments were carried out with the two single level models—the barotropic and the one-level PE. The detailed results of only a few are presented in this section. Detailed error statistics of the experiments are also given in this section.

4.1. *Flow fields*

Figs. 3 and 4 show the flow fields (streamlines and isotachs) at 700 mb for the days indicated. Here Model I refers to the barotropic model while Model II refers to the one-level PE model. The top panels (a, d, g and j) of each of Figs. 3 and 4 are the observed flow fields for each day of the indicated 4-day experiment. The middle panels (b, e, h and k) of each figure show the predicted flow fields for each day using Model I (barotropic model) while the bottom panels (c, f, i and l) depict corresponding predicted flow fields using Model II (one-level PE model).

In general, the main synoptic features of the flow fields show close agreement between the observed and the model predictions. The close agreement is better illustrated in the 24-h and 48-h fields and to some extent in the 72-h fields. In 96 h the agreement is in general not as good. The main differences between the observed and predicted fields are generally obvious at the north and south boundaries because of the boundary conditions

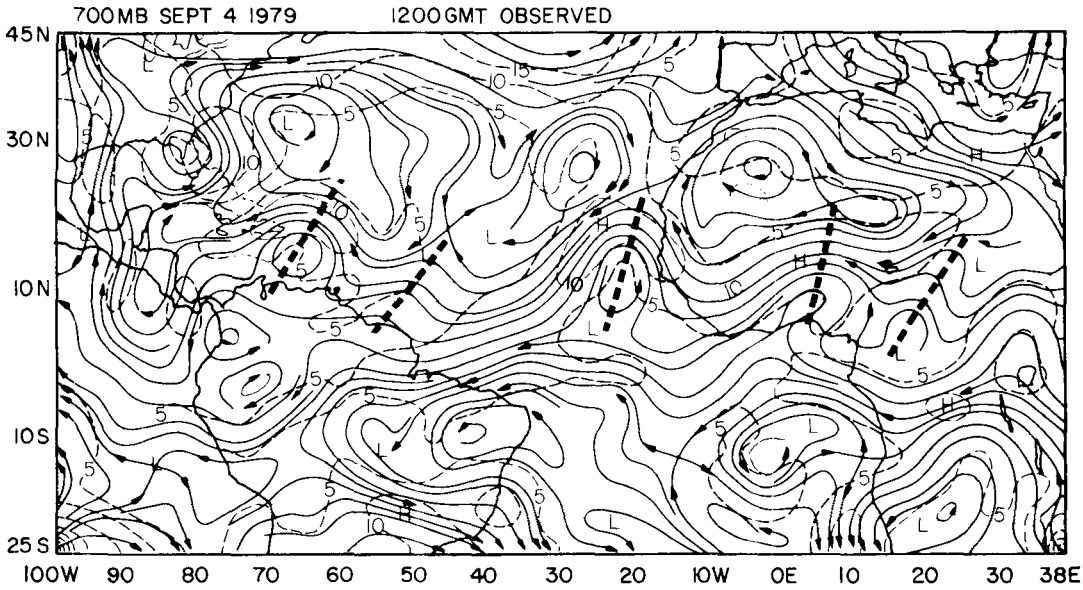

Fig. 2. Typical objectively analysed 700 mb streamlines (thin solid lines) and isotachs (thin dotted lines in units of m s^{-1}). Troughs of tropical waves are identified with heavy dashed lines: September 4, 1979 at 1200 GMT.

imposed. On the average the prediction fields of the one-level PE model seem to show smoother flow patterns especially in the trade wind areas. This is most probably because of its coarser resolution—2° mesh size—as opposed to the 1° resolution of the barotropic model.

4.2. *Atlantic tropical waves*

The heavy dark lines in the flow fields illustrated by Figs. 3 and 4 indicate the approximate trough positions of the tropical (African) waves over the Atlantic ocean. Table 3 also shows the mean values of the longitudinal trough positions of some of the waves as defined by the observed and predicted flow fields. In general, close agreement between the observed and the two predicted tropical wave trough positions exists, especially during the first 48 h. The errors in trough positions during the first 48 h average from 1° to 2° of longitude. Significant errors in trough positions (sometimes as large as 10° of longitude) have been noted between the 72 and 96 h observed and the predicted trough positions. This is mainly due to the different phase speeds of the two models. While the average phase speed of the African waves in the observed flow field for the 4 days run of each experiment is about 6·2 deg/day (or 8·0 m s^{-1}), their corresponding phase speeds for the barotropic and one-level PE model runs are approximately 5.4 deg/day (or 6.9 m s^{-1}), and 6.7 deg/day (8.6 m s^{-1}) respectively. These phase speed values show that, of the two models, the one-level PE model has a somewhat faster phase speed than the barotropic model. The main reason for this is that the wave anomaly pattern (see Fig. 1) superimposed on the initial flow field is somewhat enhanced by the convergence which is often found ahead of the wave trough position (Reed et al. 1977). Besides, it should be noted that the phase speed in the one-level PE model is also dependent on the value of the mean height of the free surface, $\bar{z}$, chosen (see paragraph 2.2.4).

4.3. *Wind speeds*

Table 4 shows the approximate values of the maximum speeds of the easterlies for the observed and model flow fields around 10° N.

In general, both the barotropic and the one-level PE models show a decay of the maximum winds by the end of each 96-h experiment. This bears out the findings of Krishnamurti et al. (1980) who also indicated that the decay is evidently due to restrictions on the boundary values of u, v and z in the models. Besides, since the kinetic energy following a parcel is not an invariant in the models,

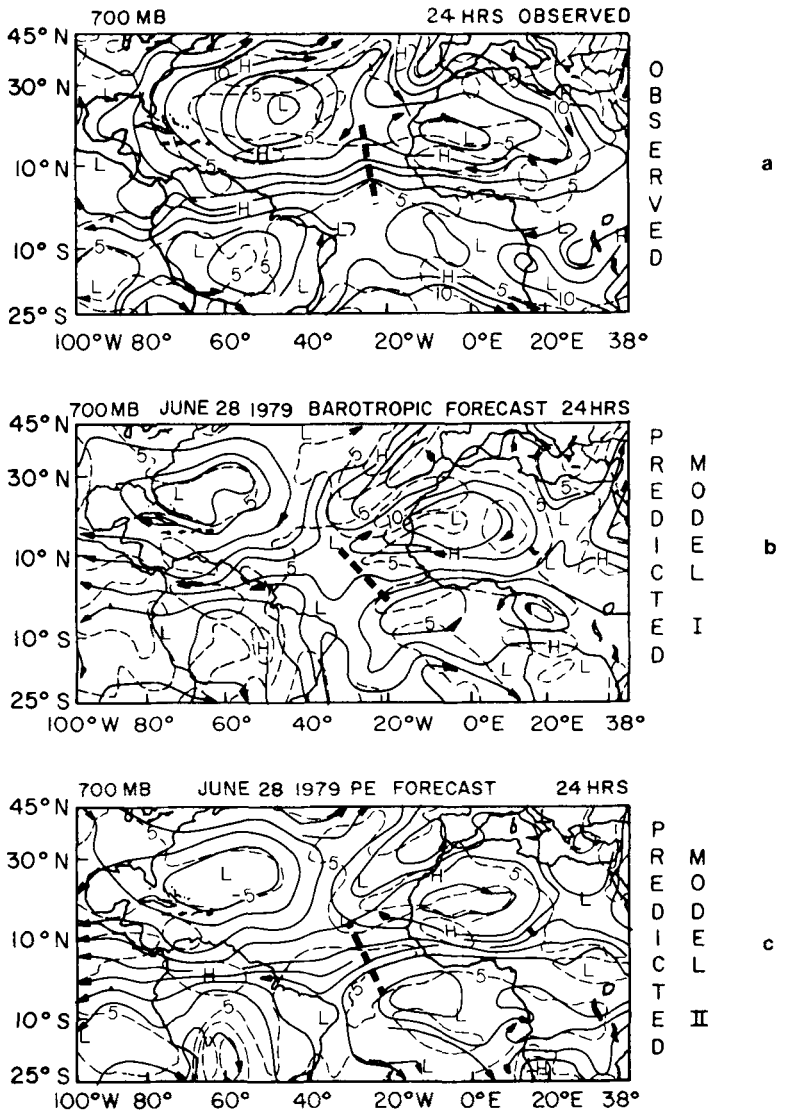

Fig. 3. The 24, 48, 72 and 96-h observed and predicted 700 mb streamlines (thin solid lines) and isotachs (thin dotted lines in units of m s^{-1}) for initial state 1200 GMT, June 28, 1979. Model I is the Barotropic Model and Model II is the One-level PE Model. The heavy dotted lines are approximate trough positions of the tropical waves. (a) Observed motion field valid at 1200 GMT, June 29, 1979, (b) 24-h barotropic forecast verifying at 1200 GMT, June 29, 1979, (c) 24-h one-level PE forecast verifying at 1200 GMT, June 29, 1979, (d) Observed motion field valid at 1200 GMT, June 29, 1979, (d) Observed motion field valid at 1200 GMT, June 30, 1979, (e) 48-h barotropic forecast verifying at 1200 GMT, June 30, 1979, (f) 48-h one-level PE forecast verifying at 1200 GMT, June 30, 1979, (g) Observed motion field valid at 1200 GMT, July 1, 1979, (h) 72-h barotropic forecast verifying at 1200 GMT, July 1, 1979, (i) 72-h one-level PE forecast verifying at 1200 GMT, July 1, 1979, (j) Observed motion field valid at 1200 GMT, July 2, 1979, (k) 96-h barotropic forecast verifying at 1200 GMT, July 2, 1979, (l) 96-h one-level PE forecast verifying at 1200 GMT, July 2, 1979.

the values of maximum winds are not expected to remain constant.

The results of the experiments also support the earlier findings of the same authors in respect to the decrease of velocity with time in the high speed regions and an increase in the low speed regions.

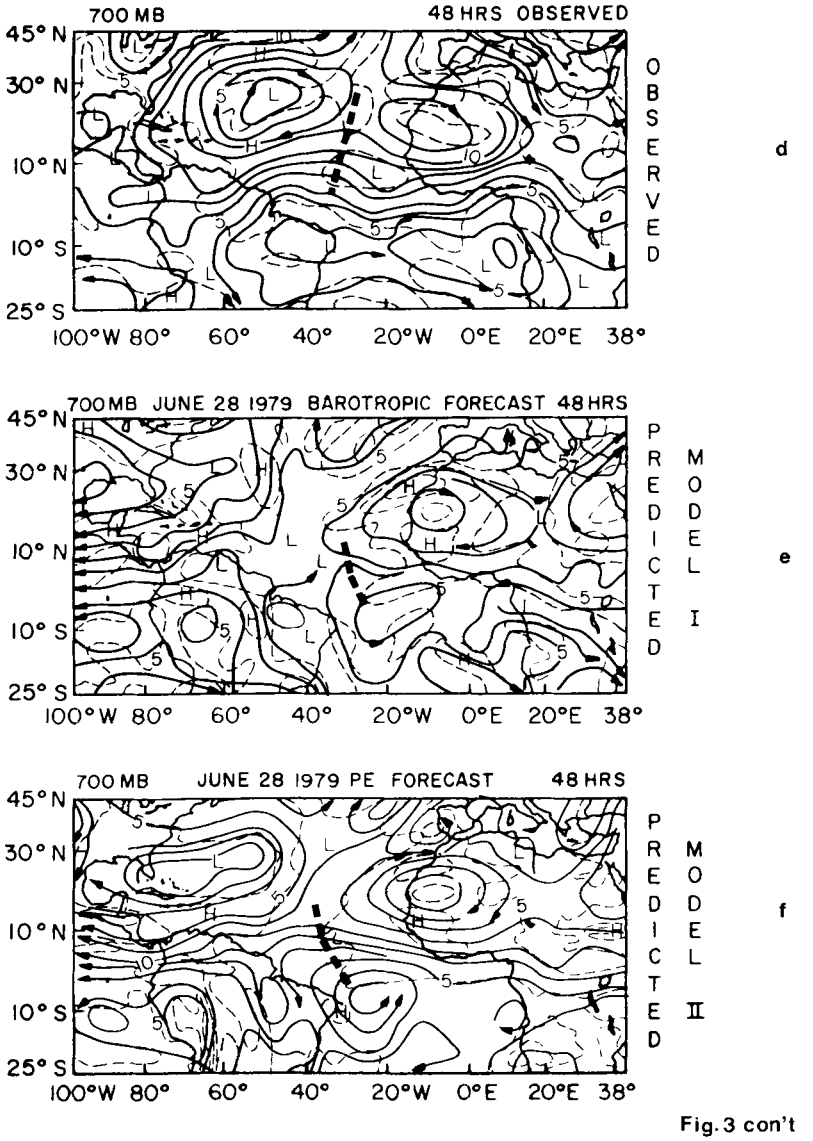

Fig. 3 con't

4.4. *Invariants*

For the 96-h runs of each of the experiments with the one-level PE model, invariants were computed each day. Table 5 illustrates the values of the mean height of the free surface, $\bar{z}$, the domain average potential vorticity, $\overline{\xi_p}$, the domain average square potential vorticity, $\overline{\xi_p^2}$, and the domain total energy, E_T, for a few of the experiments. It can be seen from these values that the invariants remained nearly constant through the 96 h in spite of the open north and south boundaries introduced into the model. Percentage departures were between 0.0 and 2.0%. This confirms the characteristics of the single level primitive equation model as earlier specified in paragraph 2.2.2.

4.5. *Verification scores*

In order to assess the degree of accuracy of the forecasts made using the single level prediction models in this study, two different types of verification scores have been computed. These are in addition to the wave trough positions already

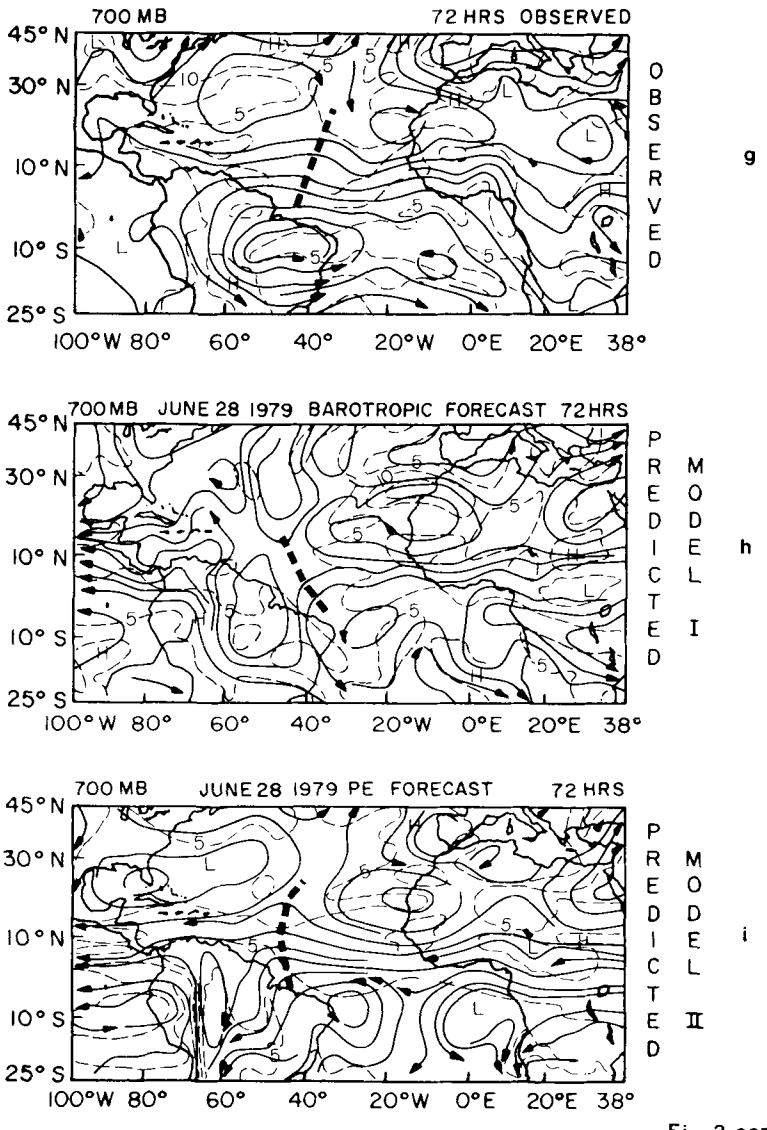

Fig. 3 con't

discussed in paragraph 4.2. These verification scores are (a) the RMS errors for the vector, zonal and meridional winds and (b) the anomaly correlation coefficient.

The RMS errors have been computed over a limited inner domain bounded by longitudes 0° and 98° W and latitudes 10° S to 30° N, while the anomaly correlation coefficient was obtained for the entire domain.

4.5.1. *RMS errors.* One good way of estimating the performance of the two forecast models used in this study is to look at the RMS vector deviation of the prediction models relative to the verification winds. Table 6 (i) shows the limited domain and time averaged RMS vector errors computed every day of each 96-h forecast for the two models compared with the results of Krishnamurti et al. (1980), Ploshay (1977) and with persistence. It is to be noted that in the tropics persistence is considered a good forecasting tool. The results show that the barotropic model performs better than persistence only in the first 48 h while the

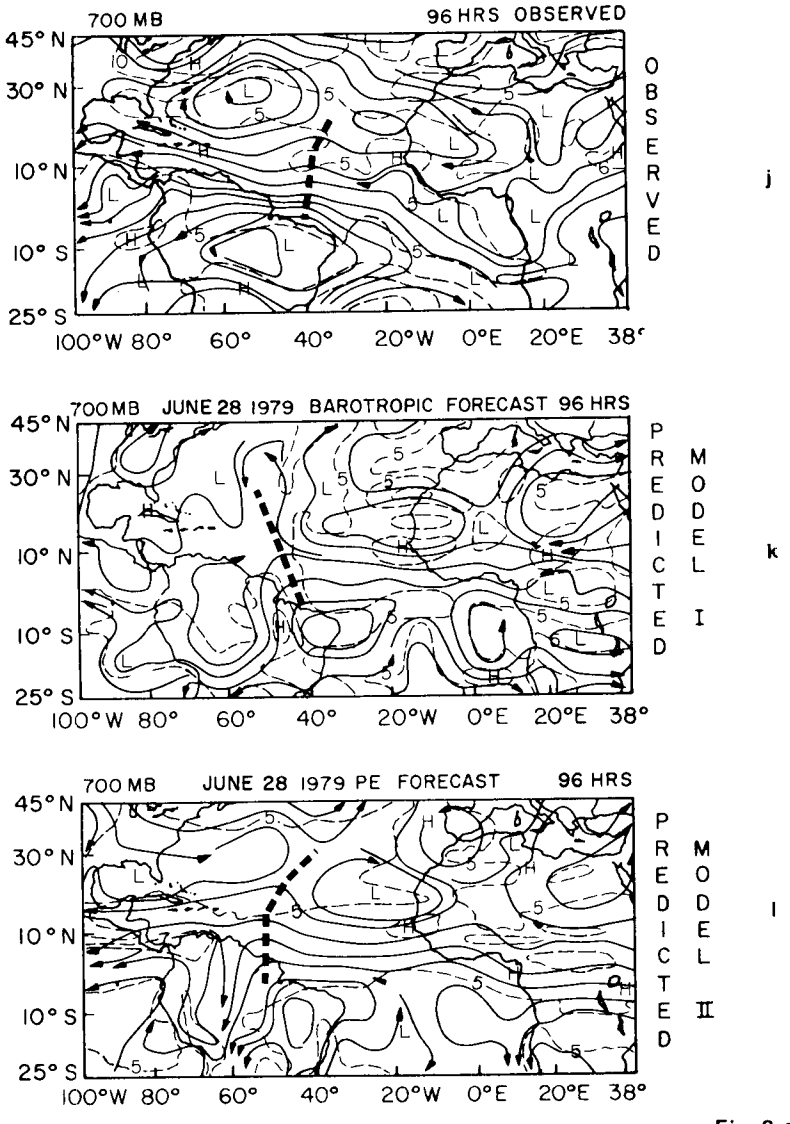

Fig. 3 con't

one-level PE model's performance in this study excels those of the barotropic model and of persistence throughout the 96 h. The results also show marked improvement over the results of Krishnamurti et al. (1980) and Ploshay (1977), who used the same models with GATE data. Tables 6 (ii) and 6 (iii) are RSM errors for the zonal (u) and meridional (v) components of the flow fields. From the tables we see that the greater errors come from the zonal flow in both models. This is most likely due to the open boundary conditions imposed in the models. The time evolution of the zonal wind (u) is dependent to some extent on values of the meridional wind (v) in the physics of the models (see eq. 2 for example).

4.5.2. *Anomaly correlation coefficient.* This skill score system has been used by the European Centre for Medium Range Weather Forecast (ECMWF) to evaluate medium range forecasts (Hollingsworth et al. 1980). The anomaly cor-

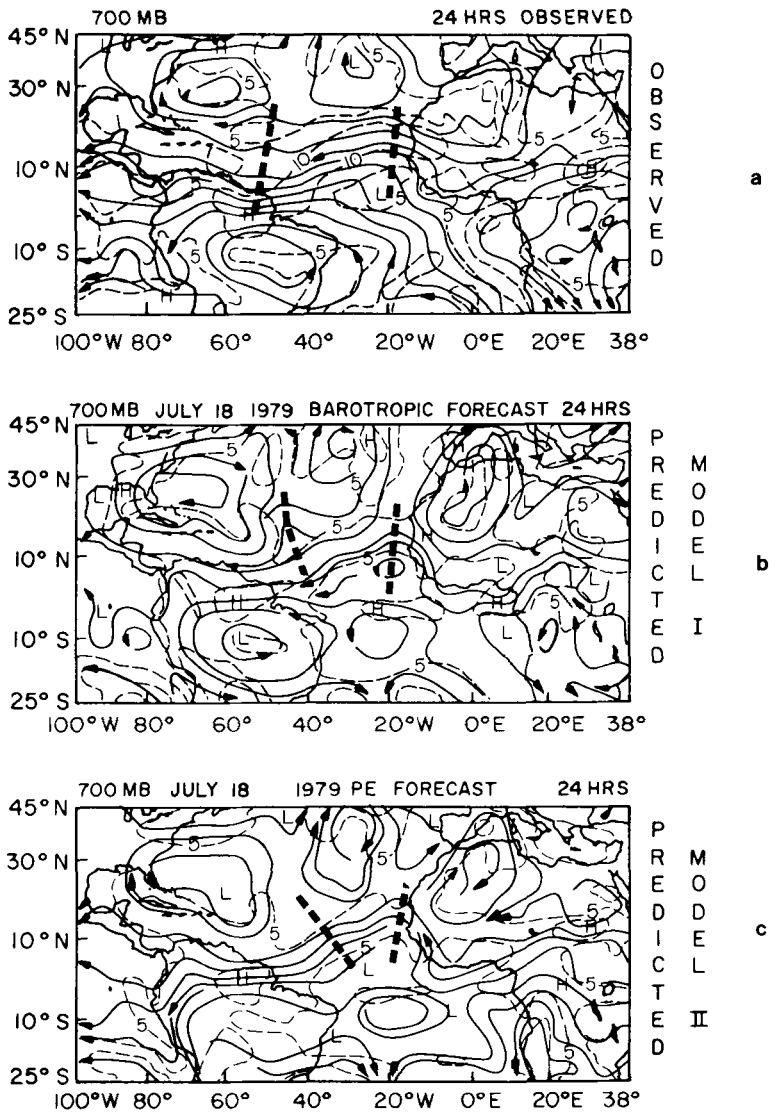

Fig. 4. The 24, 48, 72 and 96-h observed and predicted 700 mb streamlines (thin solid lines) and isotachs (thin dotted lines in units of m s^{-1}) for initial state 1200 GMT, July 18, 1979. Model I is the Barotropic Model and Model II is the one-level PE Model. The heavy dotted lines are approximate trough positions of the tropical waves. (a) Observed motion field valid at 1200 GMT, July 19, 1979, (b) 24-h barotropic forecast verifying at 1200 GMT, July 19, 1979, (c) 24-h one-level PE forecast verifying at 1200 GMT, July 19, 1979, (d) Observed motion field valid at 1200 GMT, July 20, 1979, (e) 48-h barotropic forecast verifying at 1200 GMT, July 20, 1979, (f) 48-h one-level PE forecast verifying at 1200 GMT, July 20, 1979, (g) Observed motion field valid at 1200 GMT, July 21, 1979, (h) 72-h barotropic forecast verifying at 1200 GMT, July 21, 1979, (i) 72-h one-level PE forecast verifying at 1200 GMT, July 21, 1979, (j) Observed motion field valid at 1200 GMT, July 22, 1979, (k) 96-h barotropic forecast verifying at 1200 GMT, July 22, 1979, (l) 96-h one-level PE forecast verifying at 1200 GMT, July 22, 1979.

relation coefficient is the correlation between the forecast and observed variables after the monthly normal has been subtracted. In this study, the streamfunction, ψ, is the variable used in computing the coefficient for the barotropic model experiments while the wind speeds were used in respect to

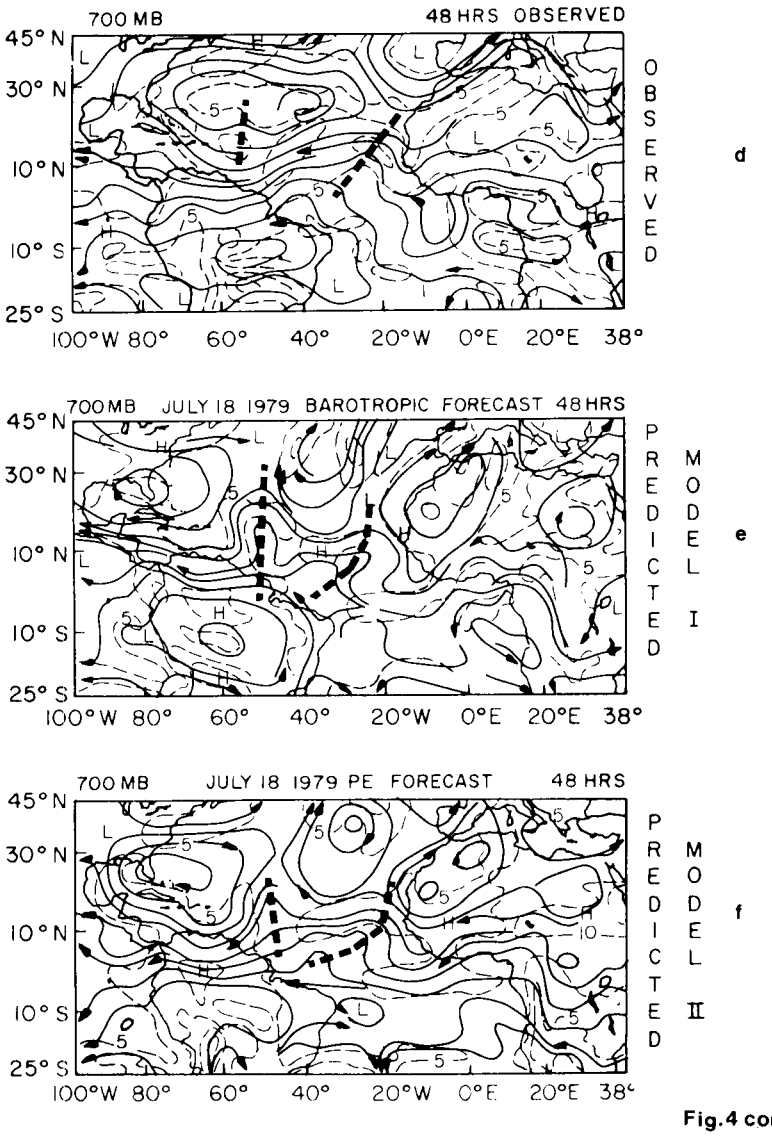

Fig.4 con't

the one-level PE model runs. Instead of the monthly normal, the mean of the daily 1200 GMT initial values of the respective variables for July 1 to September 15, 1979 has been utilized. This period is most representative of a typical African wave season.

If $X(t)$ is the value of a variable at a predicted time, t, then the anomaly is defined by:

$$\Delta X(t) = X(t) - X_n$$

where, in this study, X_n is the 77-day initial states mean. $\Delta X_p(t)$ and $\Delta X_o(t)$ are the predicted and observed values at the predicted time, t, respectively. The averaging operator $\bar{X}$ indicates an area mean.

$$\bar{X} = \frac{\sum_i g_i X_i}{\sum_i g_i}$$

where X_i is an arbitrary variable at the grid point i and g_i is a weighting factor. Here the cosine of the latitude has been used as weighting factor.

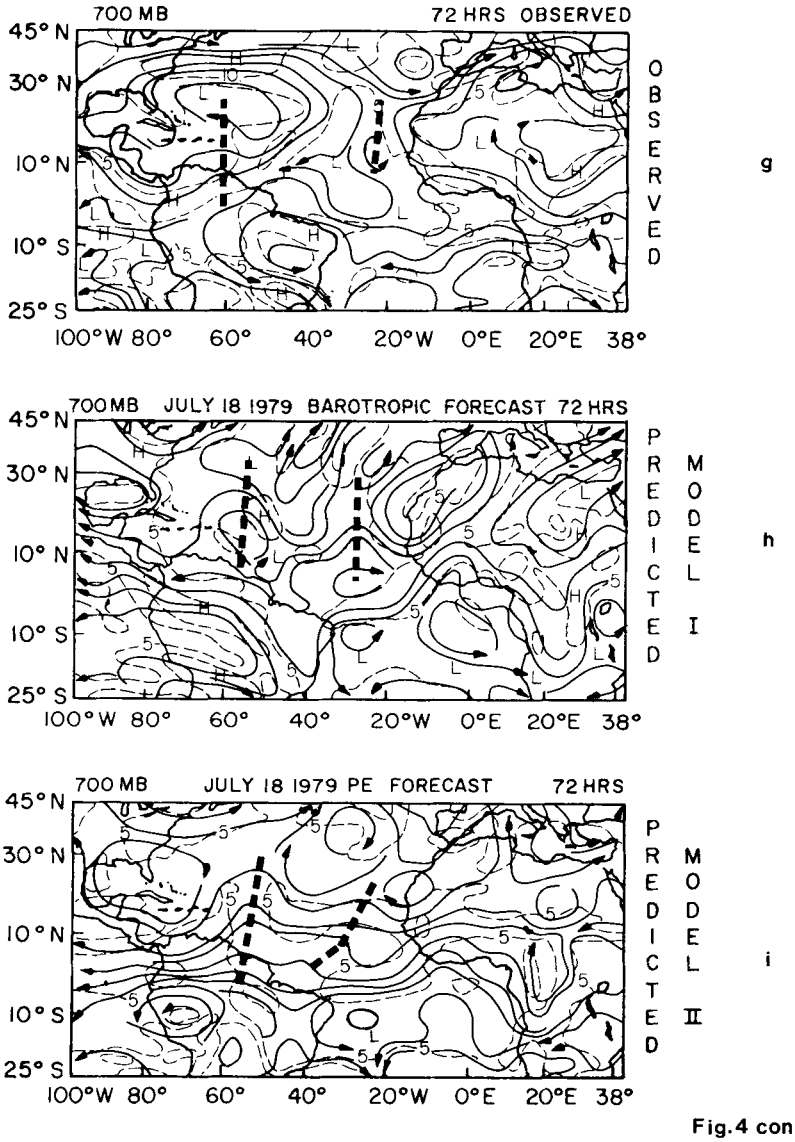

Fig.4 con't

The operator $E(X)$ is an ensemble mean of all the experiments run with each model.

$$E(X) = \frac{1}{n} \sum_{i=1}^{n} X_i$$

where X_i is the value of the anomaly correlation coefficient for each experiment and n is the number of experiments.

Anomaly correlation $= E$

$$\left(\frac{\overline{(\Delta X_p(t) - \overline{\Delta X_p(t)})\,(\Delta X_o(t) - \overline{\Delta X_o(t)})}}{\sqrt{(\Delta X_p(t) - \overline{\Delta X_p(t)})^2}\ \sqrt{(\Delta X_o(t) - \overline{\Delta X_o(t)})^2}} \right)$$

Tables 7 and 8 show the anomaly correlation coefficients between the model forecasts, barotropic and one-level PE, and verifications. From the Tables we see that the one-level PE model

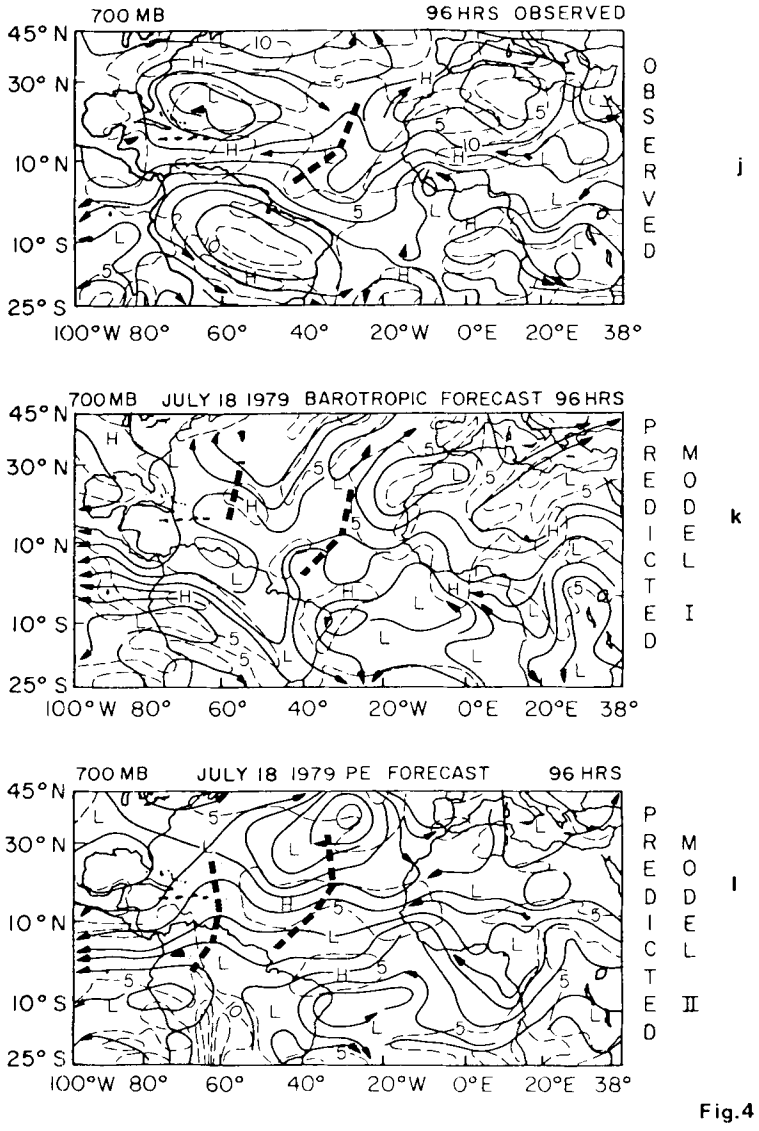

Fig.4 con't

performed better than the barotropic model throughout the 96-h period. It is also observed that both models seem to show more skill during the peak of the tropical wave season—August—than at other periods.

5. Summary and conclusion

Fifty-two 96-h prediction experiments have been carried out in this study mainly to assess the predictability over the tropics of two single level prediction models—the barotropic and the one-level PE models—that respectively use the laws of conservation of absolute and potential vortivity. The westward movement of the 700 mb Atlantic tropical waves which had originated over Central Africa are examined. In similar studies (Ploshay, 1977; Krishnamurti et al., 1980) the data set from GATE have been previously used. In the present study the data sets from the 1979 global experiment, FGGE, have been utilized.

Table 3. *Approximate positions of troughs of tropical waves*

Time of initial state		Wave	Approximate mean longitudinal position of trough											
			24 h			48 h			72 h			96 h		
	12 GMT	#	Obs	M1	M2	Obs	M1	M2	Obs	M1	M2	Obs	M1	M2
June 19, 1979	12 GMT	1	18W	18W	20W	21W	25W	31W	29W	32W	39W	33W	35W	46W
		2	25W	30W	30W	32W	34W	38W	—	42W	46W	48W	47W	51W
		3	48W	50W	52W	53W	56W	60W	53W	56W	70W	53W	72W	77W
		4	79W	80	80W	88W	86W	87W	—	92W	93W	—	97W	—
June 28, 1979	12 GMT	1	27W	27W	26W	32W	32W	37W	39W	42W	48W	41W	49W	52W
July 18, 1979	12 GMT	1	20W	20W	20W	26W	27W	26W	27W	29W	31W	32W	34W	36W
		2	50W	47W	42W	57W	52W	50W	63W	57W	56W	—	60W	62W
July 20, 1979	12 GMT	1	27W	28W	28W	32W	32W	33W	40W	37W	39W	43W	40W	45W
July 30, 1979	12 GMT	1	27W	26W	26W	42W	36W	36W	47W	40W	40W	56W	45W	45W
August 17, 1979	12 GMT	1	28W	28W	28W	38W	38W	40W	46W	46W	46W	55W	47W	53W
August 22, 1979	12 GMT	1	23W	21W	22W	31W	27W	28W	37W	30W	32W	46W	33W	37W
September 4, 1979	12 GMT	1	29W	28W	28W	36W	32W	33W	43W	33W	38W	—	38W	45W

Obs Observed; M1—Model 1 (Barotropic); M2—Model 2 (One-Level PE); A dash (—) indicates waves cannot be defined or moved out of domain.

Table 4. *Maximum speed of easterlies ($m\ s^{-1}$) around 10° N*

Time of initial state		24 h			48 h			72 h			96 h		
		Obs	M1	M2	Obs	M1	M2	Obs	M1	M2	Obs	M1	M2
June 19, 1979	12 GMT	10.2	13.5	15.0	11.6	12.8	14.2	13.7	12.5	13.5	12.3	12.4	12.1
June 28, 1979	12 GMT	13.3	13.5	11.9	13.4	13.7	12.0	13.3	12.9	11.0	10.7	13.2	12.1
July 18, 1979	12 GMT	15.1	11.1	10.4	13.7	9.7	9.6	10.5	7.7	7.6	12.6	7.7	7.4
July 20, 1979	12 GMT	10.5	11.7	11.8	12.6	10.4	10.5	14.4	10.3	10.3	15.9	10.7	9.7
July 30, 1979	12 GMT	13.4	12.6	12.2	13.6	11.0	10.9	11.2	10.3	8.9	8.87	9.6	8.2
August 17, 1979	12 GMT	12.5	12.1	12.2	11.2	11.8	13.1	9.4	13.9	14.4	12.6	12.0	14.7
August 22, 1979	12 GMT	14.0	11.7	12.6	12.5	11.9	11.1	11.2	11.8	10.8	13.7	11.0	9.5
September 4, 1979	12 GMT	10.0	12.5	11.0	10.0	11.5	11.0	13.2	9.7	11.5	12.2	8.3	10.7

Obs Observed; M1—Model 1 (Barotropic); M2—Model 2 (One-Level PE).

During the period, twenty-six of the tropical waves that moved over the Atlantic between June 16, 1979 and September 15, 1979 were investigated. The waves are those identified by Frank and Clark (1980) in their annual summary of Atlantic waves.

The results show that:

(a) The models conserved domain invariants. In particular, the one-level PE model invariants, for which statistical values have been computed (see Table 5) did not depart for more than 2% of the original value through each 96-h run. These are the domain averaged potential vorticity, square potential vorticity, mean height of the free surface and the total energy. The prediction experiments shown here used open boundaries.

(b) There exists, in general, good agreement in respect to the main synoptic features, between the predicted flow fields of the models and those of the observed, at least up to 72 h. Beyond 72 h, however, the positions of some features seem to depart considerably from the observed.

(c) The models advect the tropical waves fairly accurately for the first 48 h, the predicted trough positions are within 1° to 2° latitude of the observed. Thereafter, a deterioration in the phase speed of the waves in the barotropic model and in the one-level PE model are noted. In general, the barotropic and the one-level PE models respectively advect the tropical waves with average phase speeds of 5.4 deg/day (6.9 $m\ s^{-1}$) and 6.7 deg/day (8.6 $m\ s^{-1}$) while the

Table 5. *Domain invariants for the one-level PE model*

June 16, 1979 Hour	$\bar{z}$ (m)	ξ_p ($\times 10^{-8}$ m^{-1} s^{-1})	ξ_p^2 ($\times 10^{-16}$ m^{-2} s^{-2})	E_T ($\times 10^{-8}$ m^3 s^{-2})
24	2017.	1.142	6.863	0.2039
48	2016.	1.140	6.865	0.2036
72	2014.	1.141	6.784	0.2032
96	2012.	1.142	6.736	0.2029
% departure	0.24%	0.00%	1.85%	0.49%
July 11, 1979				
24	1996.	1.161	7.042	0.1997
48	1993.	1.155	7.011	0.1990
72	1991.	1.155	6.926	0.1986
96	1989.	1.153	6.915	0.1982
% departure	0.35%	0.69%	1.80%	0.75%
August 17, 1979				
24	1999.	1.153	6.907	0.1986
48	1989.	1.146	6.913	0.1983
72	1988.	1.142	6.852	0.1981
96	1987.	1.140	6.782	0.1979
% departure	0.6%	1.13%	1.81%	0.35%
September 4, 1979				
24	1985.	1.158	6.870	0.1976
48	1983.	1.156	6.900	0.1972
72	1981.	1.155	6.865	0.1968
96	1980.	1.153	6.795	0.1966
% departure	0.25%	0.17%	1.09%	0.51%

average observed phase speed of the waves is about 6.2 deg/day (8.0 m s^{-1}).

(d) The maximum winds in the easterlies seem to slow down somewhat in the models. This is traces to the boundary conditions imposed. At the boundaries the time evolutions of u, v, z were set to zero; this does not permit adequate middle latitude interactions.

(e) *The RMS errors (Table 6) for both models show considerable skill at 48 h; this performance is better than peristence. The performance of the one-level PE model was better than that of the barotropic model and persistence throughout the 96 h for each experiment.* The errors show an improvement over the earlier studies with the GATE data sets (Krishnamurti et al. 1980). This may be a result of the better sets of the present study. Anomaly correlation coefficients (Tables 7 and 8) were computed for both models. They show considerable skill at 24 and 48-h predictions; correlations greater than 0·5 were noted at 72 to 96 h as well. The coefficients also indicate that the performance of the one-level PE model was consistently better than the barotropic model throughout the 96-h forecasts.

The results of this series of experiments with the barotropic and the one-level PE models suggest that predictions of the movement of tropical waves over the Atlantic ocean can be carried out reasonably well up to 48 h. The predictive capability of the one-level PE model is in general

Table 6. *Root mean square error comparisons*

(i) *Vector deviation*

	Barotropic model ($m\ s^{-1}$)	One-level model ($m\ s^{-1}$)	One-level PE (Krish *et al.*, 1980) ($m\ s^{-1}$)	One-level PE (Ploshay, 1977) ($m\ s^{-1}$)	Persistence ($m\ s^{-1}$)
24 h	4.82	4.97	5.15	6.06	5.47
48 h	6.15	6.02	6.20	6.08	6.58
72 h	6.87	6.31	—	6.92	6.49
96 h	7.09	6.44	—	7.18	6.66

(ii) *Zonal wind (u) deviation*

	Barotropic model ($m\ s^{-1}$)	One-level PE model ($m\ s^{-1}$)
24 h	3.78	3.50
48 h	4.61	4.49
72 h	5.35	4.68
96 h	5.60	4.95

(iii) *Meridional wind (v) deviation*

	Barotropic model ($m\ s^{-1}$)	One-level PE model ($m\ s^{-1}$)
24 h	3.24	3.33
48 h	4.05	3.99
72 h	4.40	4.22
96 h	4.32	4.09

Table 7. *Anomaly correlation coefficient between barotropic model forecasts and verification*

Date of initial state	24 h	48 h	72 h	96 h
June 19, 1979	0.53	0.55	0.55	0.40
June 21, 1979	0.43	0.53	0.48	−0.09
June 23, 1979	0.38	0.07	0.18	0.03
June 28, 1979	0.50	0.37	0.33	0.10
June 29, 1979	0.67	0.47	0.28	0.31
July 2, 1979	0.44	0.00	−0.33	−0.11
July 11, 1979	0.64	0.40	0.21	0.05
July 18, 1979	0.48	0.62	0.52	0.55
July 20, 1979	0.70	0.69	0.47	0.59
July 30, 1979	0.65	0.57	0.60	0.46
August 13, 1979	0.66	0.69	0.52	0.66
August 17, 1979	0.72	0.63	0.80	0.66
August 19, 1979	0.80	0.78	0.68	0.71
August 22, 1979	0.77	0.65	0.69	0.34
August 25, 1979	0.58	0.79	0.62	0.54
September 4, 1979	0.64	0.67	0.38	0.66
September 7, 1979	0.64	0.54	0.20	0.55
Average	0.60	0.51	0.43	0.38

Table 8. *Anomaly correlation coefficient between one-level PE model forecasts and verifications*

Date of initial state	24 h	48 h	72 h	96 h
June 19, 1979	0.70	0.59	0.67	0.54
June 21, 1979	0.89	0.65	0.58	0.50
June 23, 1979	0.50	0.62	0.50	0.46
June 28, 1979	0.86	0.71	0.59	0.37
June 29, 1979	0.93	0.69	0.47	0.25
July 11, 1979	0.87	0.77	0.75	0.65
July 18, 1979	0.92	0.69	0.66	0.61
July 20, 1979	0.99	0.80	0.67	0.59
July 30, 1979	0.91	0.76	0.74	0.73
August 2, 1979	0.91	0.86	0.65	0.69
August 10, 1979	0.90	0.77	0.67	0.68
August 13, 1979	0.87	0.69	0.63	0.60
August 17, 1979	0.94	0.75	0.70	0.74
August 19, 1979	0.93	0.82	0.73	0.73
August 22, 1979	0.99	0.90	0.72	0.69
August 25, 1979	0.96	0.79	0.71	0.72
September 4, 1979	0.96	0.68	0.58	0.53
September 7, 1979	0.89	0.65	0.69	0.67
Total average	0.88	0.73	0.65	0.60

better than that of the barotropic model, and its 72 h forecast appears acceptable. Beyond that forecast time the predictions made with the models may not be of any operational value other than to provide a rough outlook of the flow field and trough positions. Both of these models lack physics which is necessary for the maintenance and propagation of tropical waves and that is of course a limitation. For further improvement of results one must resort to multi-level PE models where physical processes such as air–sea interaction, radiative effect, convection and condensation processes are included. Such tests with multi-level models would establish the scope of the tropical predictability problem; this again would require a large experimentation program.

6. Acknowledgements

Financial support for this work came from the National Hurricane Research Laboratory NOAA Grant No. NAB80RAD00009. Partial support for this work was also received from the National Science Foundation NSF Grant No. ATM78-19363. The Nigerian Government provided partial support for Mr. Adejokun. We wish to convey our appreciation to Dr. Stanley Rosenthal for his interest in this work.

Computational support for this work came from Florida State University and the National Center for Atmospheric Research's computing systems. The National Center for Atmospheric Research is sponsored by the National Science Foundation.

REFERENCES

Adefolalu, D. O. 1974. On scale interactions and the lower tropospheric summer easterly perturbation in West Africa. Ph.D. thesis, Department of Meteorology, Florida State University, Tallahassee, Florida 32306, USA. 275 pp.

Arakawa, A. 1966. Computational design for long term numerical integration of the equations of atmospheric motions. *J. Comp. Phys. 1*, 119–143.

Burpee, R. W. 1972. The origin and structure of easterly waves in the lower troposphere of North Africa. *J. Atmos. Sci. 29*, 77–90.

Carlson, T. N. 1969a. Synoptic histories of three African disturbances that developed into Atlantic hurricanes. *Mon. Wea. Rev. 97*, 256–276.

Carlson, T. N. 1969b. Some remarks on African disturbances and their progress over the tropical Atlantic. *Mon. Wea. Rev. 97*, 716–726.

Dunn, G. E. 1940: Cyclogenesis in the eastern Atlantic. *Bull. Am. Meteorol. Soc. 21*, 215–229.

Erickson, C. O. 1963. An insipient hurricane near the West African Coast. *Mon. Wea. Rev. 91*, 61–88.

Frank, N. L. 1970. Atlantic tropical systems of 1969. *Mon. Wea. Rev. 98*, 307–314.

Frank, N. L. and Clark, G. 1980. Atlantic tropical systems of 1979. *Mon. Wea. Rev. 108*, 966–972.

Fritz, S. 1962. Satellite pictures and the origin of hurricane Anna. *Mon. Wea. Rev. 90*, 507–513.

Gates, W. L. and Nelson, A. B. 1975. A new (revised) tabulation of Scripps Topography on a 1° global grid. Part I: Terrain heights. Rept. No. R-1276-1-ARPA—Rand Corporation, Santa Monica, California, USA.

Hockney, R. W. 1965. A fast direct solution of Poisson's equation using Fourier Analysis. *J. Am. Comp. Mech. 12*, 95–113.

Hollingsworth, A., Arpe, K., Tiedtke, M., Capaldo, M., Savijärvi, H., Åkesson, O. and Woods, J. A. 1979. Comparison of Medium Range Forecasts made with two parameterization schemes. ECMWF Tech. Report No. 13, ECMWF, Reading, England.

Krishnamurti, T. N. 1962. Numerical integration of the primitive equations by a quasi-Lagrangian advective scheme. *J. Appl. Meteorol. 1*, 508–521.

Krishnamurti, T. N. 1969. An experiment on numerical weather prediction in equatorial latitudes. *Q. J. R. Meteorol. Soc. 95*, 594–620.

Krishnamurti, T. N. and Pearce, R. P. 1977. The fundamentals of numerical weather prediction and the filtered barotropic model. Proceedings of WMO seminar, Dakar, November 1976. WMO Rept. No. 492. Geneva, Switzerland.

Krishnamurti, T. N. and Krishnamurti, R. 1979. Surface meteorology over Gate A-scale. *Deep-Sea Res. 26*, (Suppl.), 29–61.

Krishnamurti, T. N., Pan, H. L., Chang, C. B., Ploshay, J., Walker, D. and Oodally, A. W. 1979a. Numerical Weather Prediction for GATE. *Q. J. R. Meteorol. Soc. 105*, 979–1010.

Krishnamurti, T. N., Pasch, R. J. and Ardanuy, P. 1980. Prediction of African waves and specification of squall lines. *Tellus 32*, 215–231.

Mathur, M. B. 1970. A note on an improved quasi-lagrangian advective scheme for primitive equations. *Mon. Wea. Rev. 98*, 214–219.

Matsuno, T. 1966. Numerical integration of primitive equations by a simulated backward difference method. *J. Meteorol. Soc. Japan 44*, 76–84.

Pedgeley, D. E. and Krishnamurti, T. N. 1976. Structure and behavior of a monsoon cyclone over West Africa. *Mon. Wea. Rev. 104*, 149–167.

Piersig, W. 1936. Schwankungen von Luftdruck und Luftbewegung sowie ein Beitrag zum Weltergeschelen in Passat gebiet des ostidhen Nordatlantischen Ozeans. *Arch. Deut. Seewarte. 54*, No. 6 (Parts II and III have been translated—1944: The cyclonic disturbances of the Subtropical eastern North Atlantic, *Bull. Am. Meteorol. Soc. 25*, 2–18).

Ploshay, J. J. 1977. Results of single level numerical prediction experiments during GATE. Master's Thesis, Florida State University, Tallahassee, Florida 32306, USA. 88 pp.

Reed, J. R., Norquist, D. C. and Recker, E. E. 1977. The structure and properties of African Wave disturbances as observed during Phase III of GATE. *Mon. Wea. Rev. 105*, 317–333.

Thompson, R. M., Payne, S. W., Recker, E. E. and Reed, R. J. 1979. Structure and properties of synoptic-scale wave disturbances in the intertropical convergence zone of the Eastern Atlantic. *J. Atmos. Sci. 36*, 53–72.

Tripoli, G. and Krishnamurti, T. N. 1975. Low-level flows over the GATE area during summer 1972. *Mon. Wea. Rev. 103*, 197–216.

Williamson, D. L. 1976. Normal mode initialization procedure applied to forecasts with the Global shallow water equations. *Mon. Wea. Rev. 104*, 195–206.